Obrabotka metallov (tekhnologiya, oborudovanie, instrumenty) = Metal Working and Material Science. 2024 vol. 26 no. 3 pp. 135–148
ISSN: 1994-6309 (print) / 2541-819X (online)
DOI: 10.17212/1994-6309-2024-26.3-135-148

NSTU NETI

Obrabotka metallov - Metal Working and Material Science

Journal homepage: http://journals.nstu.ru/obrabotka_metallov

# Features of the use of tool electrodes manufactured by additive technologies in electrical discharge machining of products

***Timur Ablyaz*** [a], ***Vladimir Blokhin*** [b], ***Evgeniy Shlykov*** [c, *], ***Karim Muratov*** [d], ***Ilya Osinnikov*** [e]

Perm National Research Polytechnic University, 29 Komsomolsky prospekt, Perm, 614990, Russian Federation

[a] https://orcid.org/0000-0001-6607-4692, lowrider11-13-11@mail.ru; [b] https://orcid.org/0009-0009-2693-6580, warkk98@mail.ru;
[c] https://orcid.org/0000-0001-8076-0509, Kruspert@mail.ru; [d] https://orcid.org/0000-0001-7612-8025, Karimur_80@mail.ru;
[e] https://orcid.org/0009-0006-4478-3803, ilyuhaosinnikov@bk.ru

**ARTICLE INFO**

*Article history*:
Received: 11 June 2024
Revised: 25 June 2024
Accepted: 28 June 2024
Available online: 15 September 2024

*Keywords*:
Additive technologies
Selective laser melting
Copy-piercing electrical discharge machining
Current
Voltage
Pulse on time
Surface roughness
Tool electrode wear

*Funding*
The research was financially supported by the Russian Science Foundation under grant No. 23-29-00104. https://rscf.ru/project/23-29-00104/

*Acknowledgements*
The authors express their gratitude to Associate Professor of the department. ITM FSAOU VO "PNRPU" Morozov E.A. for assistance in the manufacture of samples of electrode-tools using the SLS method from maraging steel MS1.

**ABSTRACT**

**Introduction.** The paper presents the results of a study of the use of a tool electrode (*TE*), manufactured by selective laser alloying from *MS1* maraging steel powder for copy-piercing electrical discharge machining (*EDM*). **Purpose of the work:** experimental study of the features of the use of additively manufactured *TE* in the *EDM* of critical products. **Research methods.** The specimens were prepared using a *ReaLizer SLM 50* system. The starting material was spherical *MS1* powder with an average particle size of 30 μm. To test the modes and select a *TE* sample with the least number of surface defects, four manufacturing modes were tested, and the best *TE* sample was selected for further research. The *EDM* was carried out on *EMT Smart CNC* equipment in a dielectric oil environment. The specimens were installed in a clamp with straight polarity and were used as *TE*; a *0.12C-18Cr-10Ni-Ti* steel plate served as the workpiece electrode. The study was conducted using a factorial experiment (type 23) with a central design. The input data of the factorial experiment is the current $I$ (A), voltage $U$ (W), pulse on time $T_{on}$ (μs). The output parameters were the roughness parameter $Ra$ and tool electrode wear γ. The roughness parameter $Ra$ was measured using a *Mahr* Perthometer *S2*. **Results and discussion.** *TE* samples were made from *MS1* powder using the *SLS* method; the highest quality *TE* sample No. 4 was selected for *EDM*. Empirical equations are obtained that describe the relationship between the roughness parameter $Ra$ and tool electrode wear γ, depending on the *EDM* modes. At the minimum mode with a current $I = 4$ A and a voltage $U = 50$ V, the tool electrode wear is $\gamma = 0.0063875$ g. The maximum tool electrode wear is $\gamma = 0.13938$ g with a current $I = 8$ A and a voltage $U = 50$ V. It is established that at a constant pulse on time $T_{on} = 75$ μs, the smallest roughness $Ra = 2.83$ μm is obtained at a current of $I = 4$ A and a voltage $U = 100$ V, and the maximum roughness is $Ra = 4.1568$ μm at $I = 8$ A and $U = 100$ V.

**For citation:** Ablyaz T.R., Blokhin V.B., Shlykov E.S., Muratov K.R., Osinnikov I.V. Features of the use of tool electrodes manufactured by additive technologies in electrical discharge machining of products. *Obrabotka metallov (tekhnologiya, oborudovanie, instrumenty) = Metal Working and Material Science*, 2024, vol. 26, no. 3, pp. 135–148. DOI: 10.17212/1994-6309-2024-26.3-135-148. (In Russian).

*** Corresponding author**
*Shlykov Evgeniy S.*, Ph.D. (Engineering), Associate Professor
Perm National Research Polytechnic University,
29 Komsomolsky prospect,
614990, Perm, Russian Federation
**Tel.:** +7 961 759-88-49, **e-mail**: Kruspert@mail.ru

## Introduction

The relevance of the use of additive technologies in the manufacture of electrodes for electrical discharge machining (*EDM*) has arisen due to the increased requirements for the accuracy and quality of manufacturing of complex-profile products [1–3]. It has been established that one of the most rational additive methods for producing tool electrodes (*TE*) is the technology of selective laser melting (*SLM*) [4–8].

It is noted that the use of additive technologies allows to provide the required parameters of repeatable geometry of complex-profile elements, as well as to provide increased performance and durability of *TE* through the use of new compositions of powder materials. In the works [9–13] the efficiency of composite tool electrodes obtained using additive technologies is noted.

The principle of *SLM* technology is to split the product into layers and then print the product with cyclic repetition of operations. Increased requirements to accuracy, quality and reliability of product manufacturing require the use of high-quality *TE* repeating the surface profile. The required dimensional accuracy of products machined by the *EDM* method varies from 12 to 6 grades of accuracy, and the required roughness in terms of *Ra* from 3.2 to 0.8 μm. Increased requirements of accuracy and roughness are connected with operational peculiarities; machined surfaces are in conjunction with kinematic units and mechanisms.

The works [14–18] consider the *SLM* method for the production of metal tool electrodes. The authors note that the use of additive technologies for growing *TE* allows not only to provide the required parameters of repeatable geometry of complex-profile elements of products, but also to obtain increased performance and durability of *TE* by using new powder materials.

The main parameters of the *SLM* process are laser power, scanning speed, hatch type and distance, layer thickness and powder characteristics. These parameters affect the formation of defects in the process of *TE* growing. Porosity is the most frequent and difficult defect to eliminate in selective laser melting. Pore formation is influenced by the properties of the initial powder material, machine parameters and growth modes [19–21]. Another defect arising in the application of powder additive technologies is non-fusion, which occurs when single tracks do not overlap sufficiently with each other. Incorrectly selected modes for a certain material lead to increased porosity. At insufficient power value in the *SLS* process, the powder layer is not completely melted, which leads to the effect of spheroidization or non-melting with the previous layer due to the presence of unmelted particles in the track [22]. Increasing the power value leads to intensive evaporation of the material or the most fusible components of the powder, this contributes to the formation of pores. The presence of such defects contributes to the intensification of *TE* destruction in the *EDM* process. Also the presence of instability in the *TE* structure can negatively affect the formation of a stable spark formation process during copy-piercing machining, which will negatively affect the quality of processing. At present, the formed approaches to the design of *TE* configuration and assignment of machining modes rely on the methods of design of loaded critical products. These approaches do not include the peculiarities of the physical side of the *EDM* process. It is necessary to optimize the dimensions and shape of *TE* not only taking into account mass and mechanical characteristics, but also taking into account its physical properties (electrical resistance and the possibility of forming a stable spark generation channel). Initial parameters of *TE* influence the formed surface and directly the *TE* flow rate. Structural defects intensify the process of *TE* consumption in the process of *EDM*. The required surface quality is affected by the roughness of the *TE* not only before *EDM*, but also in the process itself. On this basis, it is established that ensuring the requirements of the *TE* quality is an urgent scientific and technological task.

***The purpose of the work*** is an experimental study of the application peculiarities of additively manufactured *TE* in the copy-piercing *EDM* of critical products.

***Objectives of the study are as follows:***

1) to develop a rational technique for manufacturing tool electrodes from maraging steel *MS1* using the selective laser melting method. These tool electrodes should have a minimum number of structural defects for further copy-piercing *EDM*;

2) to establish an empirical dependence of the surface quality parameter of the additively manufactured *TE* from maraging steel *MS1* depending on the modes of copy-piercing *EDM*;

3) to establish an empirical dependence of the wear of the additively manufactured *TE* from maraging steel *MS1* depending on the modes of copy-piercing *EDM*;

4) to assess the effect of the modes of copy-piercing *EDM* on the surface quality of the additively manufactured *TE* from maraging steel *MS1*.

## Research methodology

The research was carried out on the basis of the center of collective use "Center of additive technologies" of the Federal State Educational Institution of Higher Professional Education "Perm National Research Polytechnic University". Manufacturing of *TE* prototype was carried out by the additive technology method (*SLM*). Tool electrodes were made of *MS1* maraging steel powder. The powder particles had an average size of 20–40 μm and were spherical. Maraging steel are unique low-carbon martensitic steels that gain strength from intermetallic precipitates formed during the aging heat treatment process. Low carbon content provides good weldability, and significant alloying additives allow achieving high strength due to precipitation hardening mechanism. The following defects occur during the SLS process: cracks, pores, rather rough surface with the presence of melted powder particles.

It is necessary to work out fusion modes on this *MS1* powder. Carrying out trial modes will allow obtaining *TE* with a minimum number of defects.

The fusion modes were studied using the *Realizer 50* machine (Fig. 3*a*). This machine operates according to the *SLM* technology. It is used primarily for producing small-sized parts from various powders. The machine has a pulsed fiber laser. This laser has the ability to adjust the beam trajectory, as well as the duration of illumination. One of the main advantages of the *Realizer SLM 50* is the high level of detail in the products. Argon was used as a protective gas for sintering. Four modes (Table 1) of fusion of *MS1* powder material were used to obtain *TE* and the best quality one was selected.

Table 1

**Technological modes of manufacturing the tool electrode**

| No. | $t$, μs | $I$, mA | $S$, μm | $P_{av}$, W | Filling step, μm | $h$, μm | $V$, m/s |
|---|---|---|---|---|---|---|---|
| 1 | 40 | 1,400 | 20 | 35 | 0.05 | 30 | 1 |
| 2 | 40 | 1,400 | 30 | 35 | 0.05 | 30 | 0.75 |
| 3 | 20 | 1,200 | 20 | 30 | 0.05 | 30 | 1 |
| 4 | 20 | 1,400 | 20 | 35 | 0.05 | 30 | 1 |

The parameters varied during manufacturing of *TE* from the powder of *MS1* maraging steel by *SLM* method were exposure time for each point $t$, μs; operating current $I$, mA; distance between points of the laser trajectory $S$, μm; average power of laser radiation $P_{av}$, W; filling step, μm; thickness of a single layer $h$, μm; scanning speed $V$, m/s.

The samples of tool electrodes were made in the form of parallelepipeds with a length of 30 mm and a cross section of 5×5 mm. Fig. 1 shows the obtained samples on the growth substrate.


*Fig. 1.* Samples of tool electrodes

The high energy density of the *SLM* process leads to excessive material evaporation and spattering, resulting in the formation of a large number of pores. The pores reduce the fatigue characteristics and mechanical properties of the resulting products by acting as stress concentrators. Cracks on the surface of the products obtained by *SLM* methods are caused by a large temperature gradient be-

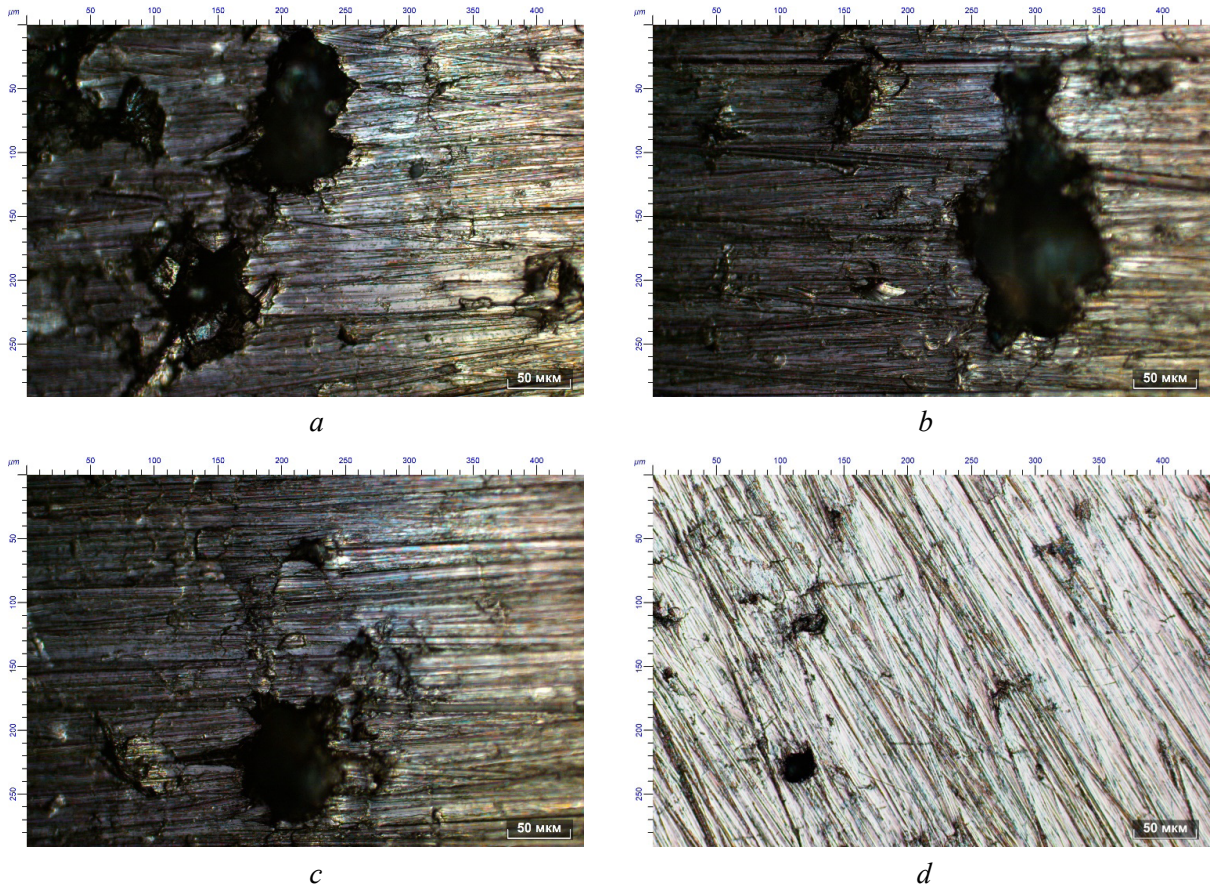


*a* *b* *c* *d*

*Fig. 2.* Surfaces of sample:
*a* – No.1; *b* – No.2; *c* – No.3; *d* – No.4

tween the melt bath and the solidified metal. On samples No.1–3 (Fig. 2*a–c*) there are chaotically arranged pores with a diameter of 40–65 μm. The surface of sample No.4 is characterized by the smallest number of structural defects (pores with a diameter of 20–28 μm, cracks up to 2–3 μm wide). When examining these samples for the presence of defects (pores, microcracks), it was found that the most suitable sample for *EDM* is No.4 (Fig. 2*d*).

Copy-piercing electrical discharge machining was carried out on an *Electronica Smart CNC machine* (Fig. 3*b*) in a transformer oil environment. The workpiece to be processed was made of stainless steel 0.12C-18Cr-10Ni-Ti. The values and range of input parameters are presented in Table 2. A *Mahr Perthometer S2* profilometer (Fig. 3*c*) was used to evaluate the surface quality parameter *Ra*. The evaluation was carried out according to the *GOST 2789-73* methodology.

The surface topography of the samples and the number of defects on its surface were assessed using an inverted metallographic microscope of the *NIM900* research class (Fig. 3*d*) at magnifications of ×300 and ×500.

In order to determine the dependencies of the formation of the roughness parameter *Ra* of *TE*, as well as the wear of the working surface of *TE*, made of *MS1* maraging steel, obtained using selective laser melting

Table 2

**Modes of copy-piercing *EDM* machining**

| Mode | Current ***I***, A | Pulse activation time $\boldsymbol{T_{on}}$, μs | Voltage ***U***, V |
|---|---|---|---|
| Minimum level | 4 | 50 | 50 |
| Medium level | 6 | 75 | 75 |
| Maximum level | 8 | 100 | 100 |

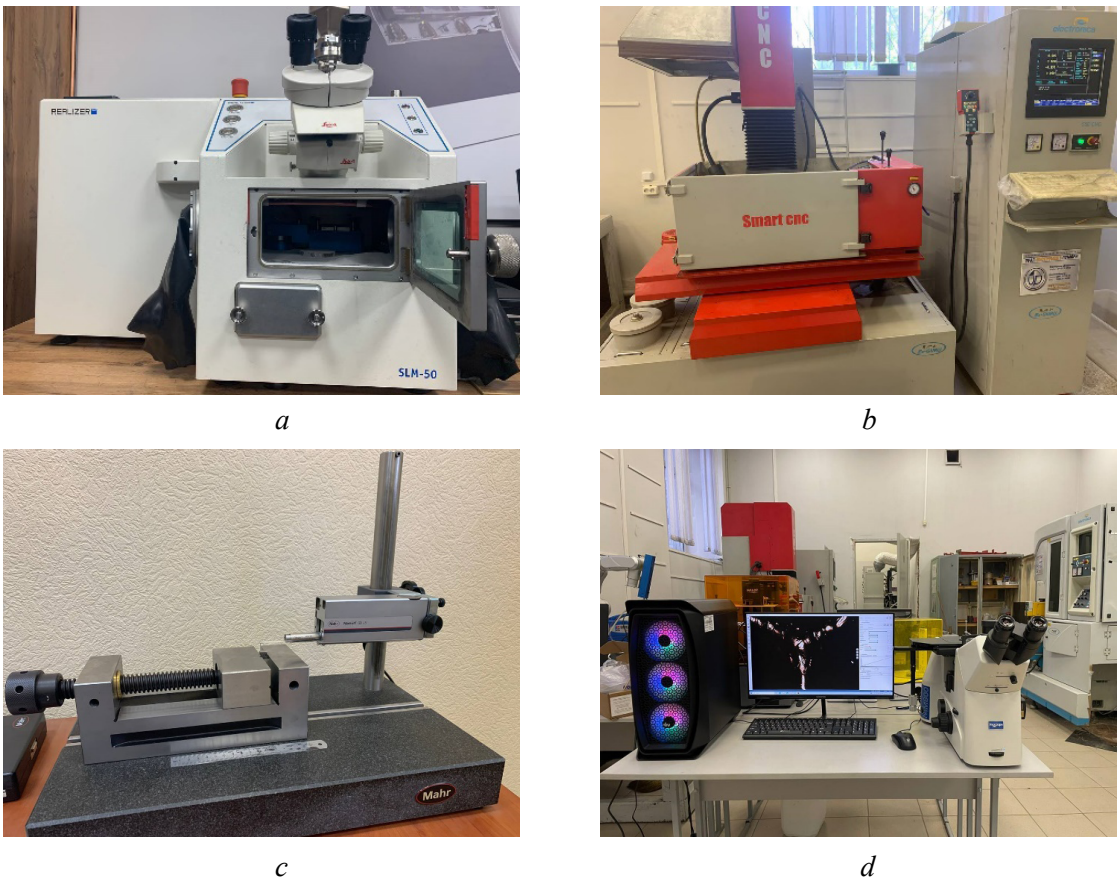


*a* *b*

*c* *d*

*Fig. 3.* Facilities for conducting the experiment and evaluating the results:
*a – ReaLizer SLM 50*; *b – NIM900* microscope; *c – Electronica Smart CNC* copy-piercing *EDM* machine; *d – Mahr Perthometer* S2 profilometer

technology, a full factor experiment (*FFE*) of type $2^3$ with the center of the plan was carried out. The factor values were coded into a matrix using transformation coordinates. The planning matrix of the experiment is shown in Table 3. The output parameters are the TE roughness parameter Ra, μm and TE wear γ, g.

The detailed methodology of *FFE* is presented in papers 23–24. According to this technique, 9 experiments were carried out and the results were obtained on the dependence of *TE* roughness *Ra* and electrode wear depending on the modes of *EDM* using *TE* manufactured by *SLS* technology from *MS1* maraging steel (Table 4).

Table 3

**Coded planning matrix**

| Exp. No. | $X_0$ | $X_1$ | $X_2$ | $X_3$ | $X_1X_2$ | $X_1X_3$ | $X_2X_3$ | $X_1X_2X_3$ |
|---|---|---|---|---|---|---|---|---|
| 1 | 1 | –1 | –1 | –1 | 1 | 1 | 1 | –1 |
| 2 | 1 | 1 | –1 | –1 | –1 | –1 | 1 | 1 |
| 3 | 1 | –1 | 1 | –1 | –1 | 1 | –1 | 1 |
| 4 | 1 | 1 | 1 | –1 | 1 | –1 | –1 | –1 |
| 5 | 1 | –1 | –1 | 1 | 1 | –1 | –1 | 1 |
| 6 | 1 | 1 | –1 | 1 | –1 | 1 | –1 | –1 |
| 7 | 1 | –1 | 1 | 1 | –1 | –1 | 1 | –1 |
| 8 | 1 | 1 | 1 | 1 | 1 | 1 | 1 | 1 |
| 9 | 1 | 0 | 0 | 0 | 0 | 0 | 0 | 0 |

Table 4

**Matrix of experimental results**

| Exp. No. | *Ra*, μm | γ, g |
|---|---|---|
| 1 | 2.9475 | 0.0062 |
| 2 | 4.33693 | 0.01 |
| 3 | 3.0374 | 0.0059 |
| 4 | 3.34163 | 0.0172 |
| 5 | 2.8057 | 0.0082 |
| 6 | 3.8035 | 0.0021 |
| 7 | 3.016 | 0.0161 |
| 8 | 4.6673 | 0.0156 |
| 9 | 3.50183 | 0.001 |

## Results and discussion

As a result of the *FFE* empirical dependencies were obtained. These dependencies establish the relationship between output parameters and processing modes. The linear relationship between the independent variable and input factors is assumed in the paper. The empirical model of the dependence of the *TE* wear parameter on the machining modes (current $\boldsymbol{I}$ (A), voltage $\boldsymbol{U}$ (W), pulse on time $\boldsymbol{T_{on}}$ (μs)), has the following form (1):

$$\gamma = 0.002997 + 0.00214325 \times I + 0.00010806 \times U - 0.00027248 \times T_{on} -$$

$$-0.00005425 \times I \times U + 0.0000028992 \times T_{on} \times U + 0.00003276 \times I \times T_{on}. \quad (1)$$

*Fisher* criterion was used to test the adequacy of the mathematical model:

$$F_{calc} = \frac{S^2_{adeq}}{S^2_y} < T_{table}, \quad (2)$$

where $F_{calc}$ and $F_{table}$ are the values of the *Fisher* criterion (respectively, calculated and tabulated); $S^2_{adeq}$ is the variance of adequacy; $S^2_y$ is the variance of reproducibility.

$$F_{calc} = 0.003 < T_{table} = 3.24. \quad (3)$$

Based on the fact that $F_{calc} < F_{table}$ at the level of dependence $\boldsymbol{\alpha} = 0.05$, we can conclude that the model satisfies the criterion of adequacy. The obtained mathematical model reliably reflects the dependence of the output parameter (wear and tear) on the modes of copy-piercing *EDM*.

Fig. 4 presents the graph of the response hypersurface. The graph establishes the dependence of input data (processing modes: $\boldsymbol{I}$, $\boldsymbol{U}$, $\boldsymbol{T_{on}}$ = 75 μs) on the *TE* wear (γ). It is established that in the minimum mode at current of $\boldsymbol{I}$ = 4 A and voltage of $\boldsymbol{U}$ = 50 V the wear of *TE* is γ = 0.0063875 g. At current of $\boldsymbol{I}$ = 8 A and voltage of $\boldsymbol{U}$ = 50 V the maximum wear of *TE* is fixed and is γ = 0.13938 g. Physical features of the character of material destruction as a result of *EDM* influence directly depend on the value of energy of a single discharge. The value of the pulse (discharge) energy increases in direct proportion with the increase of current strength. Further there is an electroerosive destruction of *TE*. At high current values, the temperature in the spark formation zone increases, which also leads to intensive wear of *TE*.

The empirical model of dependence of the surface quality parameter (roughness, *Ra*) of *TE* on processing modes (current $\boldsymbol{I}$ (A), voltage $\boldsymbol{U}$ (W), pulse on time $\boldsymbol{T_{on}}$ (μs)), has the form (4):

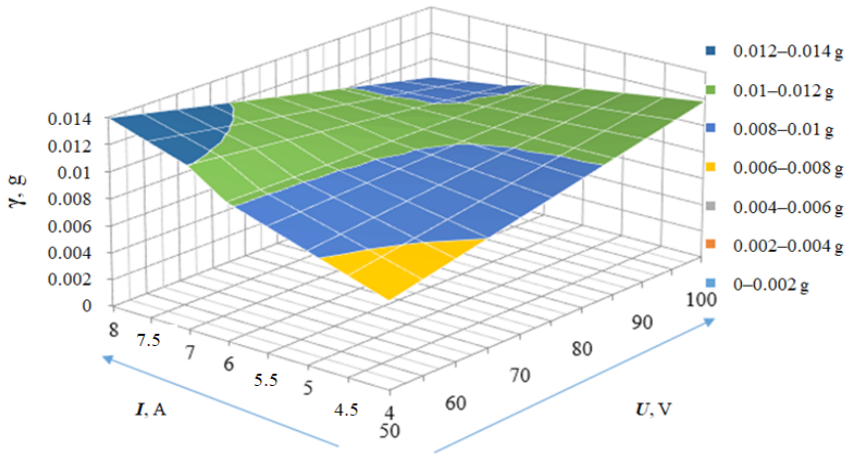


*Fig. 4.* The regression model hypersurface of electrode flow rate at constant pulse duration $T_{on}$ = 75 μs; **γ** is a tool electrode wear (g); ***I*** is a current (A); ***U*** is a voltage (V)

$$Ra = -0.7004 + 1.070300415 \times I + 0.03421764 \times U + 0.04854912 \times T_{on} -$$
$$-0.0106517 \times I \times U - 0.0006473216 \times T_{on} \times U - 0.01304028 \times I \times T_{on} +$$
$$+ 0.0001738704 \times I \times T_{on} \times U. \quad (4)$$

Fig. 5 presents a hypersurface plot showing the influence of such parameters as voltage and current on the formation of surface quality. It was found that at constant pulse turn-on time $T_{on}$ = 75 μs, the smallest *TE* roughness *Ra* = 2.83 μm was obtained at current ***I*** = 4 A and voltage ***U*** = 100 V, and the maximum *TE* surface roughness was *Ra* = 4.1568 μm at ***I*** = 8 A and ***U*** = 100 V. The values of the dimensions of the wells parameters change with the change of the power of single discharges acting in the interelectrode gap. The formation of a more accurate and clean surface of *TE* occurs at the minimum value of the power of discharges, which depend on the value of current. Increasing the current is accompanied by an increase in the depth of wells and obtaining a greater roughness of the *TE* surface.

Figures 6–8 show images of the *TE* surface after *SLM* and after copy-piercing *EDM* processing in the minimum and maximum modes. Areas of melted *MS1* powder units are observed on the surface of *TE*

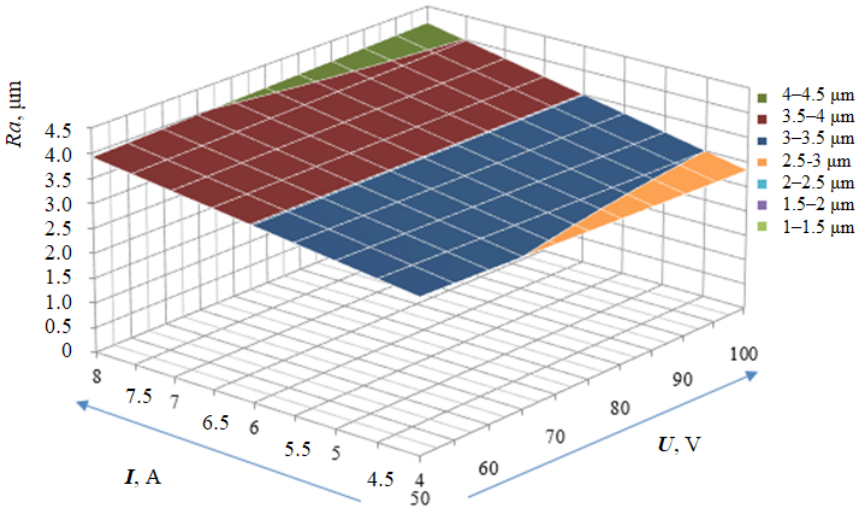


*Fig. 5.* The regression model hypersurface of the *TE* surface roughness at constant pulse on time $T_{on}$ = 75 μs; ***Ra*** is the roughness parameter (μm); ***I*** is a current (A); ***U*** is a voltage (V)

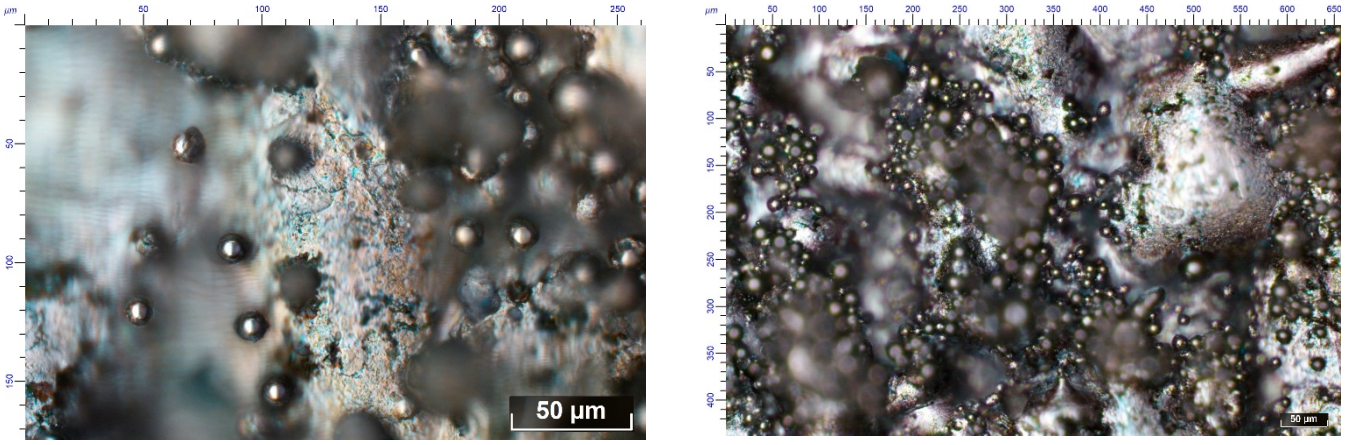


*a* *b*

*Fig. 6.* Electrode surface before machining (after 3D printing) at magnifications of ×500 (*a*) and ×300 (*b*)

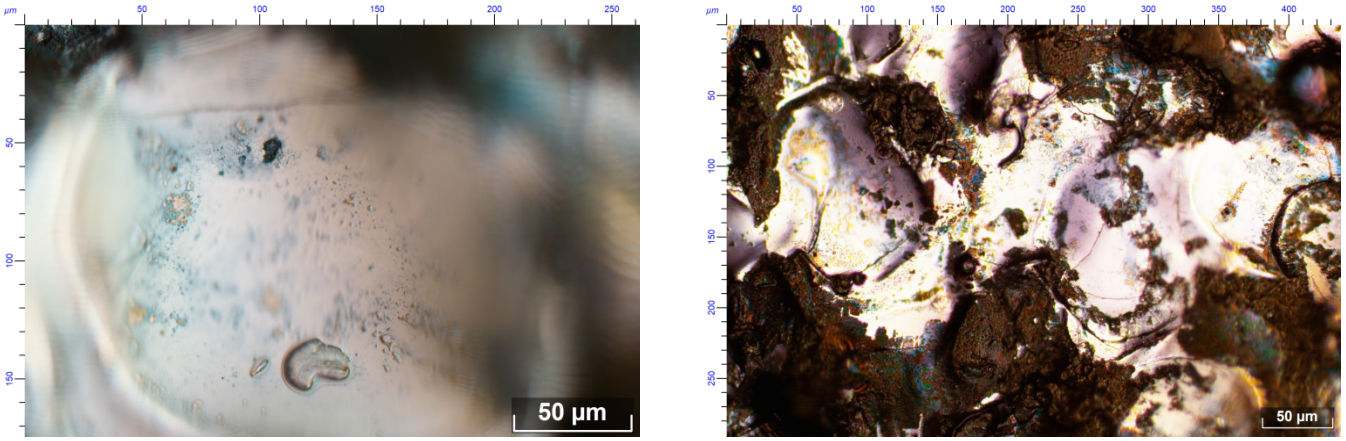


*a* *b*

*Fig. 7.* Electrode surface after electrical discharge machining at minimum mode at magnification ×500 (*a*) and ×300 (*b*)

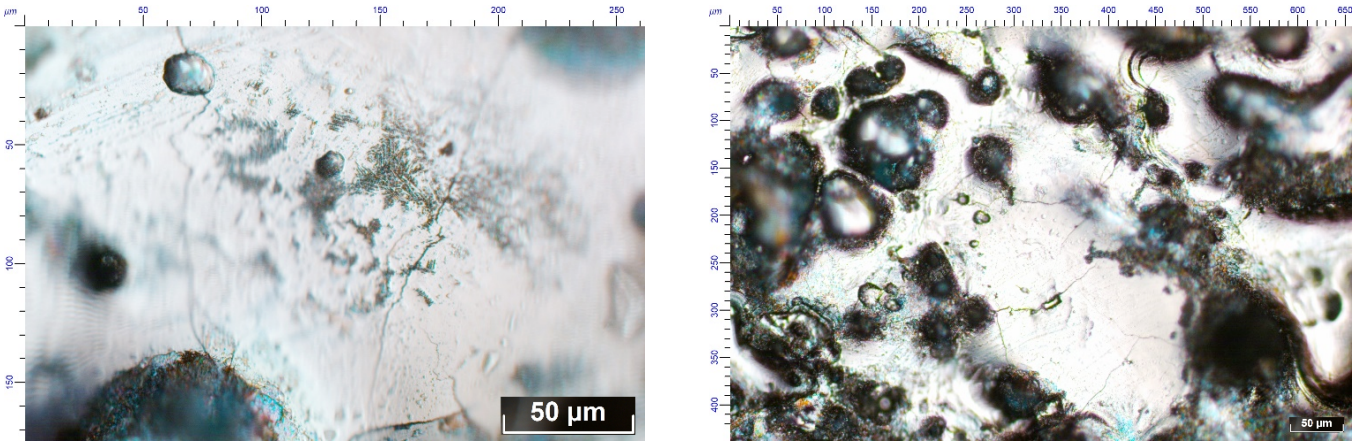


*a* *b*

*Fig. 8.* Electrode surface after electrical discharge machining at maximum mode at magnification ×500 (*a*) and ×300 (*b*)

(Fig. 6) made of maraging steel *MS1* by *SLM* method. It was found that the melted areas are located chaotically on the *TE* surface. Pores between the melted areas are also observed. After *EDM*, the surface of *TE* acquires a smooth and even morphology. With copy-piercing *EDM* in the maximum modes at $\boldsymbol{I}$ = 8 A, $\boldsymbol{T_{on}}$ = 100 µs, $\boldsymbol{U}$ = 100 V, hollows and chaotic cracks are formed, accompanied by zones of melted material

(Fig. 7–8). With copy-piercing *EDM* at $\boldsymbol{I}$ = 8 A, $\boldsymbol{T_{on}}$ = 100 μs, $\boldsymbol{U}$ = 100 V, the presence of chaotic cracks up to 1–3 μm wide was found (Fig. 8). Cracks on the *TE* surface arise due to rapid heating of the surface (with the increase of the current value and pulse on time the temperature in the processing zone increases) and rapid cooling by dielectric liquid. Hollows on the surface of the electrode after copy-piercing *EDM* are associated with the accumulation of sludge from the products of destruction of the electrode material and detail electrode (*DE*). With the increase of current and pulse activation time the intensification of the fracture process occurs. Material melt zones appear with increasing energy of single pulses (with an increase in current).

The *EDM* process is accompanied by high temperatures at the breakdown spot. Rapid heating and subsequent cooling cycles cause thermal stresses on the *TE* surface. These stresses contribute to the formation of cracks on the *TE* surface. The presence of microcracks and other surface defects leads to macro-defects of the surface layer and to a decrease in the operational properties of the *TE*. The topology of the machined surface of additively grown *TE*, shown in Fig. 7*a* at magnification ×500, shows that to exclude surface defects of *TE* it is required to use the minimum mode of copy-piercing *EDM* at current of $\boldsymbol{I}$ = 4 A, voltage of $\boldsymbol{U}$ = 100 V.

## Conclusions

Tool electrodes were produced by selective laser melting from *MS1* maraging steel powder. It is found that tool electrode sample No.4 contains a minimum number of pores and cracks. It was produced using a single point exposure time of 20 μs; operating current of 1,400 mA; distance between points of 20 μm; average laser power of 35 W; filling step of 0.05 μm; thickness of a single layer of 30 μm; scanning speed of 1 m/s.

A regression dependence between modes of copy-piercing *EDM* and wear of tool electrode when machining *TE* from maraging steel is obtained. In the minimum mode with a current of $\boldsymbol{I}$ = 4 A and a voltage of $\boldsymbol{U}$ = 50 V the wear of the electrode is minimal and amounts to $\boldsymbol{\gamma}$ = 0.0063875 g. The maximum wear of the electrode-tool amounts to $\boldsymbol{\gamma}$ = 0.13938 g with a current of $\boldsymbol{I}$ = 8 A and a voltage of $\boldsymbol{U}$ = 50 V.

A regression dependence between modes of copy-piercing *EDM* and the surface roughness quality parameter of the additively grown *TE* made of *MS1* maraging steel is obtained. It is shown that at constant pulse on time $\boldsymbol{T_{on}}$ = 75 μs the smallest roughness of *TE Ra* = 2.83 μm is obtained at a current of $\boldsymbol{I}$ = 4 A and a voltage of $\boldsymbol{U}$ = 100 V, and the maximum roughness of the *TE Ra* = 4.1568 μm is obtained at $\boldsymbol{I}$ = 8 A and $\boldsymbol{U}$ = 100 V.

It is established that on the surface of additively grown *TE* from *MS1* maraging steel there are chaotically located surface defects (microcracks, hollows, broken sections and remelting zones), reducing the strength characteristics of *ET*. To exclude surface defects and to form a homogeneous surface it is necessary to use finishing modes with the value of current $\boldsymbol{I}$ = 4 A, voltage $\boldsymbol{U}$ = 100 V and pulse turn-on time $T_{on}$ = 75 μs. It is established that with increasing values of current up to 8 A in the interelectrode gap there is an increase in temperature and the value of pulse discharge, which leads to structural defects.

## References

1. Rajurkar K.P., Sundaram M.M., Malshe A.P. Review of electrochemical and electrodischarge machining. *Procedia CIRP*, 2013, vol. 6 (2), pp. 13–26. DOI: 10.1016/j.procir.2013.03.002.

2. Dimla D.E., Hopkinson N., Rothe H. Investigation of complex rapid EDM electrodes for rapid tooling applications. *The International Journal of Advanced Manufacturing Technology*, 2004, vol. 23 (3), pp. 249–255. DOI: 10.1007/s00170-003-1709-8.

3. Ho K.H., Newman S.T. State of the art electrical discharge machining (EDM) // *International Journal of Machine Tools and Manufacture*. 2003. Vol. 43 (13), pp. 1287–1300. DOI: 10.1016/S0890-6955(03)00162-7.

4. Ayesta I., Flaño O., Izquierdo B., Sanchez J.A., Plaza S. Experimental study on debris evacuation during slot EDMing. *Procedia CIRP*, 2016, Vol. 42, pp. 6–11. DOI: 10.1016/j.procir.2016.02.174.

5. Uhlmann E., Polte J., Bolz R., Yabroudi S., Streckenbach J., Bergmann A. Application of additive manufactured tungsten carbide-cobalt electrodes with interior flushing channels in S-EDM. *Procedia CIRP*, 2020, vol. 95, pp. 460–465. DOI: 10.1016/j.procir.2020.03.136.

6. Uhlmann E., Bergmann A., Bolz R., Gridin W. Application of additive manufactured tungsten carbide tool electrodes in EDM. *Procedia CIRP*, 2018, vol. 68, pp. 86–90. DOI: 10.1016/j.procir.2017.12.027.

7. Rathi M.G., Mane D.V. An overview of additive mixed EDM. *International Journal of Scientific and Research Publications*, 2014, vol. 4 (11), pp. 1–6.

8. Batista M.D., Chandrasekaran S., Moran B.D., Troya M.S. Design and additive manufacturing of optimized electrodes for energy storage applications. *Carbon*, 2023, vol. 205, pp. 262–269. DOI: 10.1016/j.carbon.2023.01.044.

9. Gu D., Shen Y., Xiao J. Influence of processing parameters on particulate dispersion in direct laser sintered WC–Co p/Cu MMCs. *International Journal of Refractory Metals and Hard Materials*, 2008, vol. 26 (5), pp. 411–422. DOI: 10.1016/j.ijrmhm.2007.09.005.

10. Grisharin A.O., Ogleznev N.D., Muratov K.R., Ablyaz T.R. Investigation of the machinability of composite materials electrode-tools while EDM. *IOP Conference Series Materials Science and Engineering*, 2019, vol. 510 (1), pp. 1–5. DOI: 10.1088/1757-899X/510/1/012006.

11. Singh P., Sidhu S.S., Payal H.S. Fabrication and machining of metal matrix composites: a review. *Materials and Manufacturing Processes*, 2015, vol. 31 (5), pp. 1–21. DOI: 10.1080/10426914.2015.1025976.

12. Thakur A., Pabla B.S. Surface modification using composite electrodes in EDM: a review. *International Journal for Research in Applied Science and Engineering Technology*, 2023, vol. 11 (10), pp. 1008–1013. DOI: 10.22214/ijraset.2023.56134.

13. Amorim F.L., Czelusniak T., Higa C.F., Lohrengel A. Development and application of new composite materials as EDM electrodes manufactured via selective laser sintering. *The International Journal of Advanced Manufacturing Technology*, 2014, vol. 72, pp. 9–12. DOI: 10.1007/s00170-014-5765-z.

14. Amorim F.A., Lohrengel A., Muller N., Schafer G., Czelusniak T. Performance of sinking EDM electrodes made by selective laser sintering technique. *The International Journal of Advanced Manufacturing Technology*, 2012, vol. 65, pp. 9–12. DOI: 10.1007/s00170-012-4267-0.

15. Nyamekye P., Nieminen P., Bilesan M.R., Repo E., Piili H., Salminen A. Prospects for laser based powder bed fusion in the manufacturing of metal electrodes: a review. *Applied Materials Today*, 2021, vol. 23, pp. 1–20. DOI: 10.1016/j.apmt.2021.101040.

16. Weber J., Wain A.J., Piili H., Vuorema A. Residual porosity of 3D-LAM-printed stainless steel electrodes allows galvanic exchange platinisation. *ChemElectroChem*, 2016, vol. 3 (6), pp. 1–24. DOI: 10.1002/celc.201600098.

17. Sahu A.K., Mahapatra S.S. Performance analysis of tool electrode prepared through laser sintering process during electrical discharge machining of titanium. *The International Journal of Advanced Manufacturing Technology*, 2020, vol. 106 (6), pp. 1017–1041. DOI: 10.1007/s00170-019-04675-1.

18. Jiang Y., Kong L., Yu J., Hua C. Experimental research on preparation and machining performance of porous electrode in electrical discharge machining. *Journal of Mechanical Science and Technology*, 2022, vol. 36 (1–3), pp. 1–15. DOI: 10.1007/s12206-022-1134-2.

19. Zhang B., Li Y., Bai Q. Defect formation mechanisms in selective laser melting: a review. *Chinese Journal of Mechanical Engineering*, 2017, vol. 30 (3), pp. 515–527. DOI: 10.1007/s10033-017-0121-5.

20. Cao S., Chen Z., Yang K., Lim S.C.V. Defect, microstructure, and mechanical property of Ti-6Al-4V alloy fabricated by high-power selective laser melting. *JOM: The Journal of the Minerals, Metals & Materials Society*, 2017, vol. 69 (12). – P. 2684–2692. DOI: 10.1007/s11837-017-2581-6.

21. Li R., Liu J., Shi Y., Wang L. Balling behavior of stainless steel and nickel powder during selective laser melting process. *The International Journal of Advanced Manufacturing Technology*, 2012, vol. 59 (9), pp. 1025–1035. DOI: 10.1007/s00170-011-3566-1.

22. Promoppatum P., Yao S.C. Analytical evaluation of defect generation for selective laser melting of metals. *The International Journal of Advanced Manufacturing Technology*, 2019, vol. 103, pp. 1–4. DOI: 10.1007/s00170-019-03500-z.

23. Ablyaz T.R., Shlykov E.S., Muratov K.R., Zhurin A.V. Study of the EDM process of bimetallic materials using a composite electrode tool. *Materials*, 2022, vol. 15 (3), pp. 1–13. DOI: 10.3390/ma15030750.

24. Ablyaz T.R., Shlykov E.S., Muratov K.R. Improving the efficiency of electrical discharge machining of special-purpose products with composite electrode tools. *Materials*, 2021, vol. 14 (20), pp. 1–19. DOI: 10.3390/ma14206105.

## Conflicts of Interest

The authors declare no conflict of interest.

© 2024 The Authors. Published by Novosibirsk State Technical University. This is an open access article under the CC BY license (http://creativecommons.org/licenses/by/4.0).